Electronic Supplementary Material (ESI) for Journal of Materials Chemistry C.

Electronic Supporting Information

Perovskite hybrid solar cells with the fullerene derivative electron extraction layer

Wenzhan Xu,[a,b] Xiang Yao,[b] Tianyu Meng, [a] Kai Wang,[a] Fei Huang,[b] Xiong Gong[a,b,*] and Yong Cao[b]

[a] Department of Polymer Engineering, College of Polymer Science and Polymer Engineering, The University of Akron, OH 44325, United States

[b] Institute of Polymeric Optoelectronics, State Key Laboratory of Luminescent Materials and Devices, South China University of Technology, Guangzhou 510640, P. R. China

*Corresponding author, E-mails: xgong@uakron.edu, Fax: (330) 9723046

List of Figures

Fig.S1 Histograms of photovoltaic parameters for pero-HSCs W/$PC_{61}BM$ EEL and pero-HSCs W/$PC_{61}BM$-Py EEL: a) PCE, b)V_{OC}, c)J_{SC}, and d)FF

Fig.S2 AFM tapping-mode height images and corresponding phase images of (a and d) $CH_3NH_3PbI_3$, (b and e) $CH_3NH_3PbI_3$/$PC_{61}BM$ and (c and f) $CH_3NH_3PbI_3$/$PC_{61}BM$-Py thin films

Fig. S3 Top-view scanning electron microscopy images of $PC_{61}BM$ on top of perovskite films

Fig. S4 The J-V curve of electron-only devices under illumination

Fig. S5 Light intensity dependence of J_{SC}

Fig. S6 XRD pattern of ITO/PEDOT:PSS/ $CH_3NH_3PbI_3$/$PC_{61}BM$ and $PC_{61}BM$-Py EEL

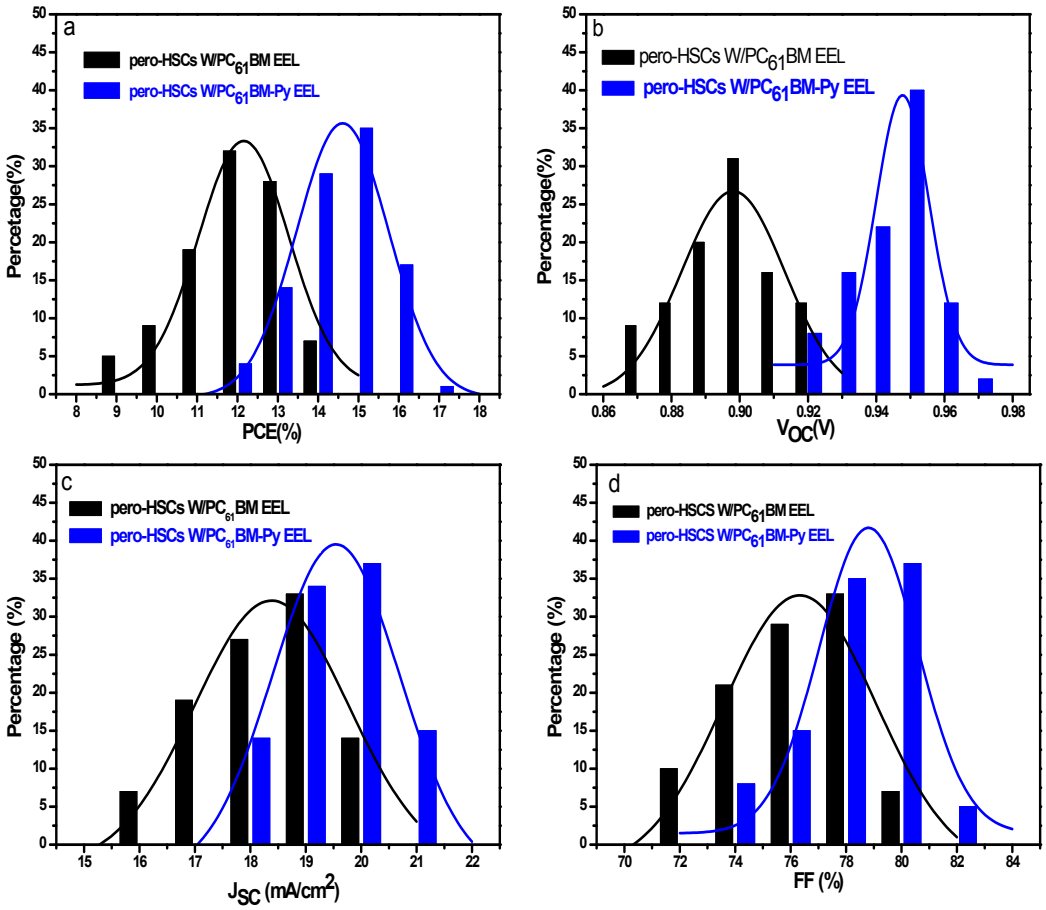

Fig. S1 Histograms of photovoltaic parameters for pero-HSCs W/PC_{61}BM EEL and pero-HSCs W/PC_{61}BM-Py EEL: a) PCE, b)V_{OC}, c)J_{SC}, and d)FF

According to the results showed in Fig. S1, it is concluded that the photovoltaic parameters of the pero-HSCs incorporated with the PC_{61}BM-Py EEL have a smaller standard deviation in comparison to those of the pero-HSCs incorporated with the pristine PC_{61}BM EEL.

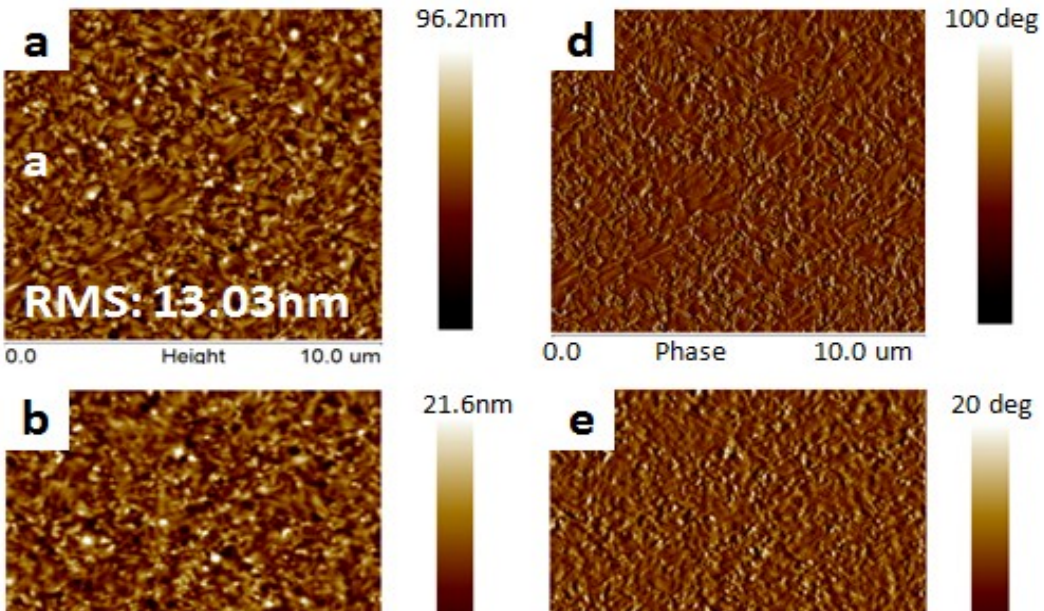

Fig. S2 AFM tapping-mode height images and corresponding phase images of (a and d) $CH_3NH_3PbI_3$, (b and e) $CH_3NH_3PbI_3/PC_{61}BM$ and (c and f) $CH_3NH_3PbI_3/PC_{61}BM$-Py thin films.

According to the height image, the AFM images showed that the root-mean-square (RMS) value of $PC_{61}BM$ layer was reduced, indicating the surface of $PC_{61}BM$ becomes smoother. The RMS of $CH_3NH_3PbI_3$ films is 13.03 nm. However, after $PC_{61}BM$ coated on the top of $CH_3NH_3PbI_3$ films, the RMS of the $CH_3NH_3PbI_3/PC_{61}BM$ thin film is significantly decreased to 2.95 nm. And the RMS of the $CH_3NH_3PbI_3/PC_{61}BM$-Py thin film is reduced to 2.71 nm. The smooth surface of the $CH_3NH_3PbI_3/PC_{61}BM$-Py layer would facilitate the electron being transported from the $CH_3NH_3PbI_3/PC_{61}BM$-Py layer to BCP layer and being collected by Ag electrode, resulting in high J_{SC} and large FF, thus high PCEs

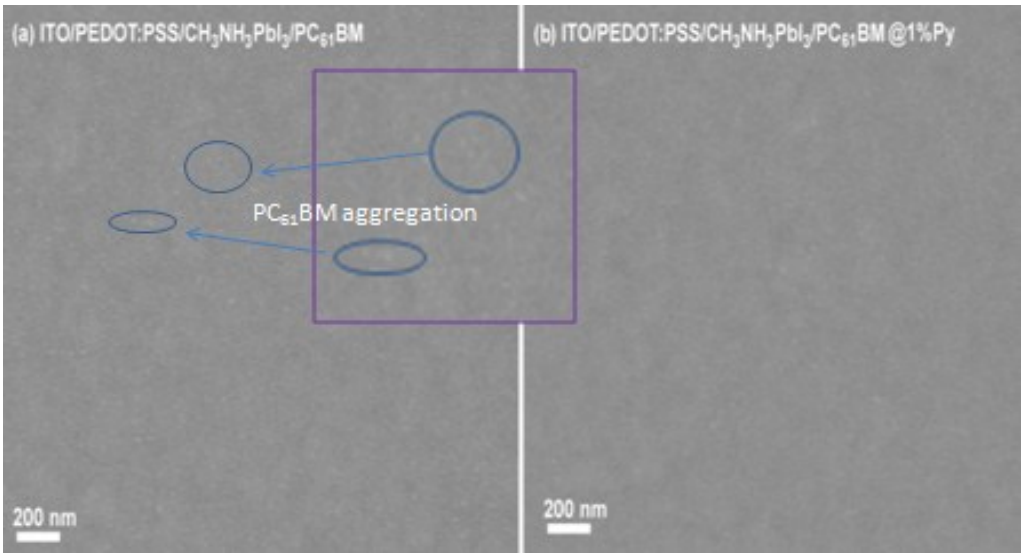

Fig. S3 Top-view scanning electron microscopy images of $PC_{61}BM$ on top of perovskite films.

Fig. S3 presents the top SEM images of the $CH_3NH_3PbI_3/PC_{61}BM$ layer and the $CH_3NH_3PbI_3/PC_{61}BM$-Py layer. Reduced aggregation of $PC_{61}BM$ molecules is observed from the $CH_3NH_3PbI_3/PC_{61}BM$-Py layer, which indicates the molecular packing of $PC_{61}BM$ is more condense.

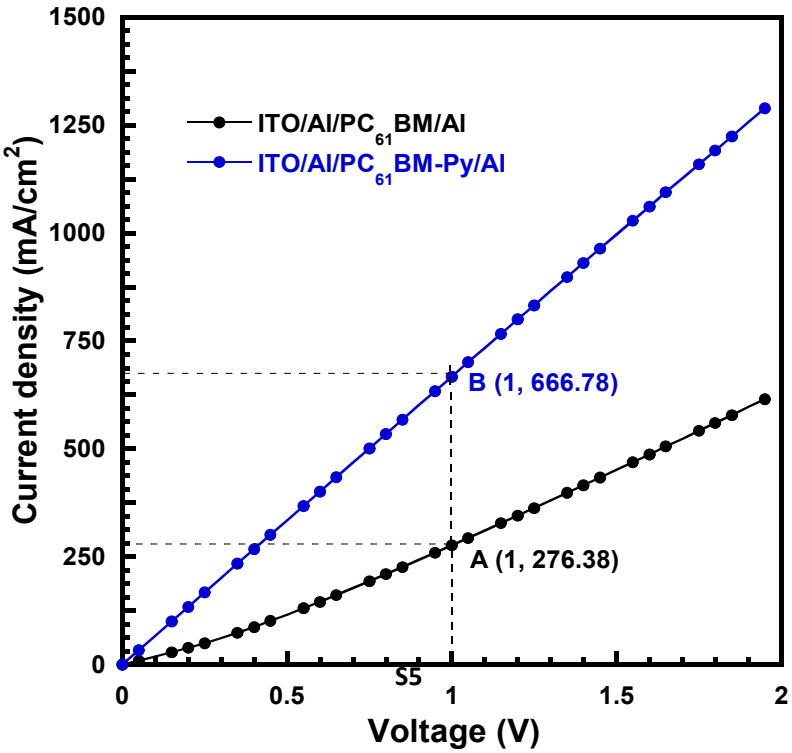
1500
1250
1000
750
500
250
0
Current density (mA/cm^2)
ITO/Al/PC$_{61}$BM/Al
ITO/Al/PC$_{61}$BM-Py/Al
B (1, 666.78)
A (1, 276.38)
0
0.5
1
1.5
2
Voltage (V)

S5

Fig. S4 The J-V curve of electron-only devices under illumination.

It is found that the $PC_{61}BM$-Py EEL possesses more than 2-fold enhanced current densities as compared with those of the $PC_{61}BM$ EEL at the same applied voltage, which illustrates that improved charge transporting properties of the $PC_{61}BM$-Py EEL

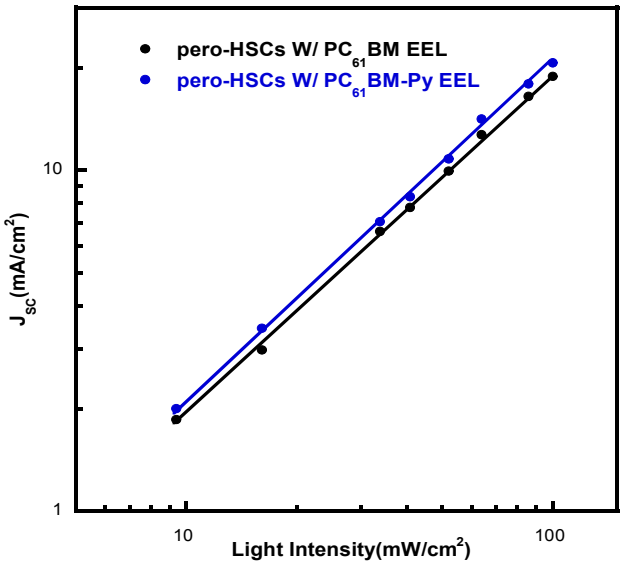

Fig. S5 light intensity dependence of J_{SC}

According to the power-law: Jsc $\propto I^{\alpha}$, with α= 0.94 and α= 0.98 are observed from the

pero-HSCs with $PC_{61}BM$ EEL and the pero-HSCs with $PC_{61}BM$-Py EEL, respectively. Based on the device physics of solar cells, a large α indicates that there is less bimolecular recombination in cells. Thus, we conclude that the $PC_{61}BM$-Py EEL can reduce the bimolecular recombination in the pero-HSCs.

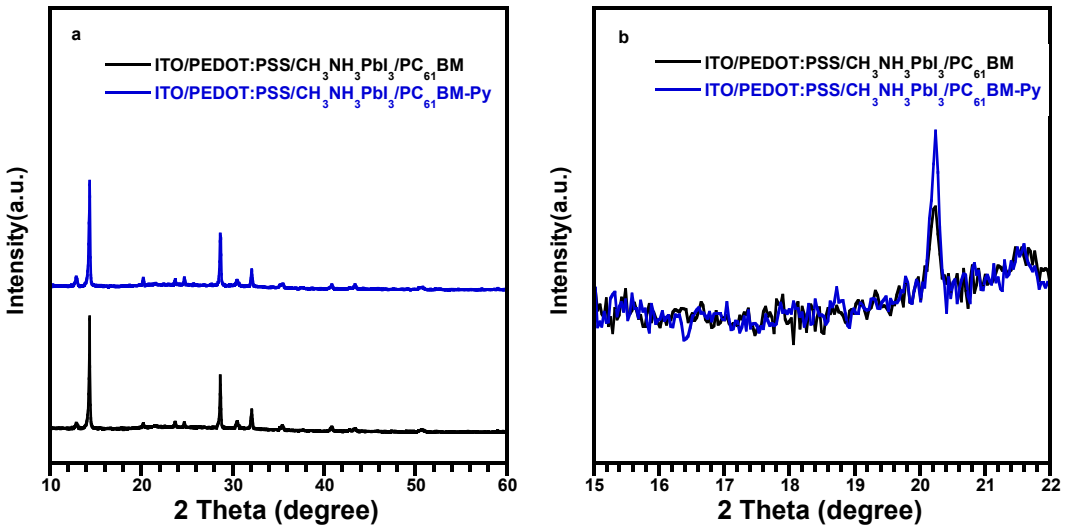

Fig. S6 XRD pattern of ITO/PEDOT:PSS/ $CH_3NH_3PbI_3/PC_{61}BM$ and $PC_{61}BM$-Py EEL.

The XRD patterns have showed that the intensity of the peak, corresponding to $PC_{61}BM$ is

increased for the $PC_{61}BM$-Py thin film, as compared with that for pristine $PC_{61}BM$ layer. The enhanced peak intensity indicates that a high crystallinity is formed in the $PC_{61}BM$-Py thin film.